

Mixed-ligand Complexes of Copper(II). I. An ESR Study of Coordination Bonding¹⁾

Hiroshi YOKOI, Masaki OTAGIRI, and Taro ISOBE

Chemical Research Institute of Non-aqueous Solutions, Tohoku University, Katahira, Sendai

(Received January 13, 1971)

The sample solutions were prepared by mixing equal volumes of any two of the 1.00×10^{-2} mol/l solutions of the 1:2 complexes of copper(II) with ethylenediamine, *N,N*-dimethylethylenediamine, *N,N*-diethylethylenediamine, 1,3-diaminopropane, L-alanine, L-serine, *N,N*-diethylglycine, and β -alanine, where an equivolume mixture of water and methanol was used as the solvent. The X-band ESR measurements for these sample solutions were carried out at the temperature of liquid nitrogen. The observed ESR line shapes showed that only the mixed-ligand complexes are formed almost quantitatively in all the solutions except two: equivolume mixtures of the two complex solutions of ethylenediamine and β -alanine and those of ethylenediamine and *N,N*-dimethylglycine, in which the coexistence of two or more complex species was clearly demonstrated. The ESR line shapes and, furthermore, the intensities of the visible absorption indicated that the symmetry of the ligand field of the mixed-ligand complexes is as axial as that of the parent complexes. The ESR experimental results showed that the $g_{//}$ value of a mixed-ligand complex almost equals the mean of the $g_{//}$ values of its two parent complexes, but that there is not such a clear correlation between their $A_{//}$ values. It was interestingly concluded from the determined g values that the covalency of the metal-ligand bonds of a mixed-ligand complex are intermediate in degree between those of its two parent complexes.

Studies of mixed-ligand complexes from various angles have become very important in recent years, since mixed-ligand complexes occur during transition states of metal-ion-catalyzed reactions,²⁾ since they are important in analytical chemistry,³⁾ and since they can be regarded as models for metalloenzyme-substrate complexes.^{4,5)} Investigations of their stability in solutions, furthermore, are considered to be important in establishing a more advanced theory as to the stability of metal-ion complexes. Most studies of mixed-ligand complexes have so far been concerned with their stability.^{6–10)}

Recently, Farona *et al.* published a paper about the coordination bonding of mixed-ligand complexes, an investigation where various β -diketone chelate complexes of copper(II) were prepared and studied by the infrared, visible absorption, and ESR methods in connection with the parent complexes.¹¹⁾ The ESR

technique is effective in obtaining useful information about coordination, namely, about the strength and symmetry of the ligand field, in copper(II) complexes.¹²⁾ The purpose of this paper is to investigate more systematically the coordination of mixed-ligand complexes in connection with that of the parent complexes, using the ESR method, and using as the parent complexes the 1:2 chelate complexes of copper(II) with ethylenediamine, its alkyl derivatives, 1,3-diaminopropane, and various amino acids.

Experimental

Materials. The sample complexes, which were used as parent complexes in this study, were prepared according to the methods in the literature,^{13,14)} were recrystallized from water or methanol, and were identified by elemental analysis.^{15–17)} They are listed in Table 1. All of the reagents used were commercially available.

ESR and Optical Measurements. 1.00×10^{-2} mol/l solutions of the complexes listed in Table 1 were prepared by using an equivolume mixture of water and methanol as the solvent. These solutions were directly used as the samples of the parent complexes themselves, while equal volumes of any two of them were mixed and used as the samples of the mixed-ligand complexes. The ESR spectra of these samples were measured at the temperature of liquid nitrogen with a Hitachi X-band ESR spectrometer, Model MES-4001, equipped with a 100 kHz field modulation unit. The field was calibrated with an NMR probe and then with a benzene solution of vanadyl acetylacetonate. Some of the observed ESR spectra are shown in Figs. 1–4. The optical absorption spectra were measured at room temperature for the same sample solutions with a Hitachi spectrophotometer, Model

1) Preliminary report of this series: H. Yokoi, M. Otagiri, and T. Isobe, This Bulletin, **44**, 1445 (1971).

2) J. P. Collman and D. A. Buckingham, *J. Amer. Chem. Soc.*, **85**, 3039 (1963); D. A. Buckingham, J. P. Collman, D. A. R. Happer, and L. G. Marzilli, *ibid.*, **89**, 1082 (1967); A. Nakahara, K. Hamada, Y. Nakao, and T. Higashiyama, *Coordin. Chem. Rev.*, **3**, 207 (1968).

3) A. K. Babko, *Talanta*, **15**, 721 (1968); R. M. Dagnall, M. T. El-Ghamry, and T. S. West, *ibid.*, **15**, 1353 (1968); B. W. Bailey, J. E. Chester, R. M. Dagnall, and T. S. West, *ibid.*, **15**, 1359 (1968).

4) A. Goudot, "Mécanique Ondulatoire et Biologie Moléculaire," ed. by L. de Broglie, *Revue D'optique Théorique et Instrumentale*, Paris (1961), p. 45.

5) A. S. Mildvan and M. Cohn, *J. Biol. Chem.*, **241**, 1178 (1966); E. J. Peck, Jr. and W. J. Ray, *ibid.*, **244**, 3754 (1969).

6) J. I. Watters and E. D. Longham, *J. Amer. Chem. Soc.*, **75**, 4919 (1953); J. I. Watters, J. Mason, and A. Aaron, *ibid.*, **75**, 5212 (1953); R. Dewitt and J. I. Watters, *ibid.*, **76**, 3810 (1954).

7) S. Kida, This Bulletin, **29**, 805 (1956).

8) S. Kida, *ibid.*, **34**, 962 (1961).

9) H. Sigel, Proc. 3rd Symp. "Coordination Chemistry," Debrecen, Hungary, 1970, Vol. 1, ed. by M. T. Beck, Akadémiai Kiado, Budapest (1970), p. 191.

10) Y. Marcus and I. Eliezer, *Coordin. Chem. Rev.*, **4**, 273 (1969).

11) M. F. Farona, D. C. Perry, and H. A. Kuska, *Inorg. Chem.*, **7**, 2415 (1968).

12) B. R. McGarvey, "Transition Metal Chemistry," Vol. 3, ed. by R. L. Carlin, Marcel Dekker, New York (1967), p. 89.

13) P. Pfeiffer and H. Glasser, *J. Prakt. Chem.*, **151**, 134 (1938).

14) E. Abderhalden and E. Schnitzler, *Z. physiol. Chem.*, **163**, 94 (1927).

15) H. Yokoi and T. Isobe, This Bulletin, **41**, 2835 (1968).

16) H. Yokoi and T. Isobe, *ibid.*, **42**, 2187 (1969).

17) H. Yokoi, M. Sai, T. Isobe, and S. Ohsawa, to be published.

TABLE 1. PARENT COMPLEXES

Ligand	Abbr.	Copper(II) complex	No. of solution ^{a)}
Ethylenediamine	en	[Cu(en) ₂](ClO ₄) ₂	I
<i>N,N</i> -Dimethylethylenediamine	dmen	[Cu(dmen) ₂](ClO ₄) ₂	II
<i>N,N</i> -Diethylethylenediamine	deen	[Cu(deen) ₂](ClO ₄) ₂	III
1,3-Diaminopropane	tn	[Cu(tn) ₂](ClO ₄) ₂	IV
L-Alanine	L-Ala ^{b)}	[Cu(L-Ala) ₂]	V
L-Serine	L-Ser ^{b)}	[Cu(L-Ser) ₂]	VI
<i>N,N</i> -Dimethylglycine	dmg ^{b)}	[Cu(dmg) ₂]·3H ₂ O	VII
β -Alanine	β -Ala ^{b)}	[Cu(β -Ala) ₂]·6H ₂ O	VIII

a) 1.00×10^{-2} mol/l, Solvent: an equivolume mixture of water and methanol.

b) Those ligands represent the anions.

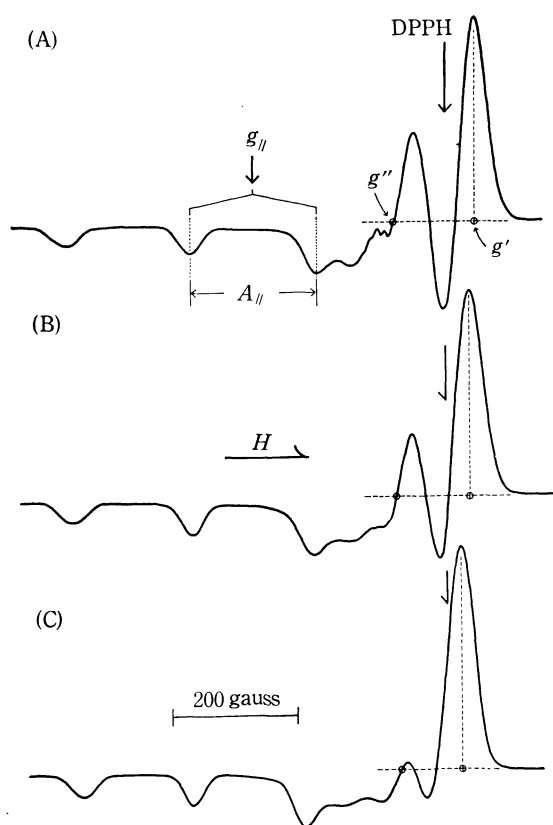


Fig. 1. The X-band ESR spectra of solution samples (measured at 77°K, Solvent: an equivolume mixture of water and methanol).

(A) the 1.00×10^{-2} mol/l solution of [Cu(en)₂]²⁺

(B) the equivolume mixture of the (A) and (C) solutions

(C) the 1.00×10^{-2} mol/l solution of [Cu(deen)₂]²⁺

EPS-3T. All the visible absorption spectra consisted of a single broad band; therefore, only the wavelengths of maximum absorption, λ_{\max} , and the molecular extinction coefficients are listed in Tables 2 and 3.

Results and Discussion

Complex Species in Solution. When two kinds of copper(II) complexes with bidentate ligands are dissolved to make a solution, the following equilibrium is generally established in the solution:⁶⁻⁸⁾

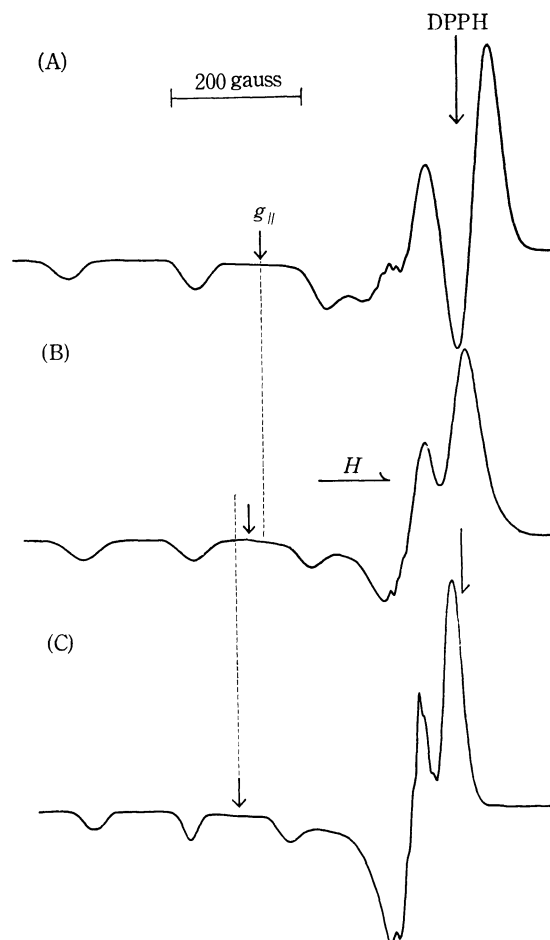
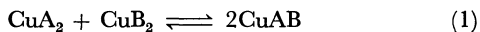


Fig. 2. The X-band ESR spectra of solution samples (measured at 77°K, Solvent: an equivolume mixture of water and methanol).

(A) the 1.00×10^{-2} mol/l solution of [Cu(en)₂]²⁺

(B) the equivolume mixture of the (A) and (C) solutions

(C) the 1.00×10^{-2} mol/l solution of [Cu(L-Ala)₂]

$$K = \frac{[\text{CuAB}]^2}{[\text{CuA}_2][\text{CuB}_2]} \quad (2)$$

where CuA₂ and CuB₂ represent parent complexes, and CuAB, a mixed-ligand complex. The relative amounts of the three complexes in the solution, therefore, vary according to the *K* value.

The ESR line shape of a single complex species of copper(II) complexes in the rigid solution has been

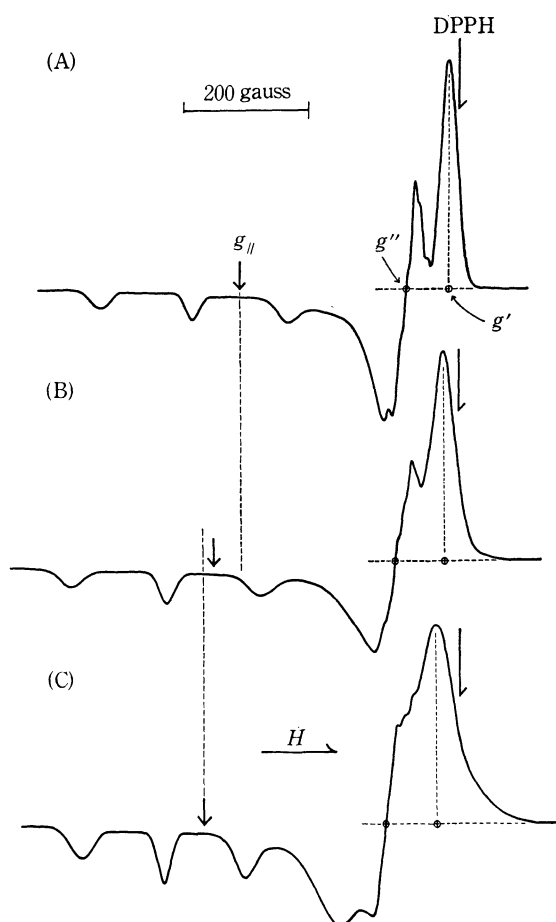


Fig. 3. The X-band ESR spectra of solution samples (measured at 77°K, Solvent: an equivolume mixture of water and methanol).

- (A) the 1.00×10^{-2} mol/l solution of $[\text{Cu}(\text{L-Ala})_2]$
 (B) the equivolume mixture of the (A) and (C) solutions
 (C) the 1.00×10^{-2} mol/l solution of $[\text{Cu}(\beta\text{-Ala})_2]$

studied by several authors.^{18,19} If two different complex species of copper(II) complexes coexist independently in the solution, the observed ESR spectrum will be made up of the superposition of their individual ESR spectra. Judging from the line shape, the ESR spectra of (B) in Figs. 1—3 can be said to be almost all due to a single complex species; furthermore, the absorption lines are different in position from those of the parent complexes. It can, therefore, be concluded that almost all the (B) spectra of Figs. 1—3 are due to mixed-ligand complexes; only mixed-ligand complexes are formed quantitatively in these systems. Such is the case with all the other sample solutions except two. The ESR spectra of these two exceptional solutions are shown in Fig. 4; the details in these cases will be discussed in the next paper of this series.²⁰ The line shapes in Fig. 4 clearly demonstrate that two or more complex species coexist in these solutions; this can, in short, be attributed to the comparatively small K values. However,

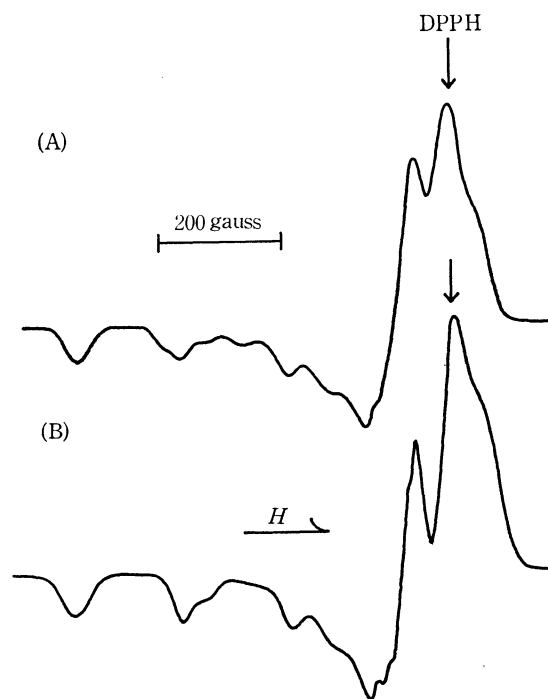


Fig. 4. The X-band ESR spectra of solution samples (measured at 77°K, Solvent: an equivolume mixture of water and methanol).

- (A) the equivolume mixture of the 1.00×10^{-2} mol/l solutions of $[\text{Cu}(\text{en})_2]^{2+}$ and $[\text{Cu}(\beta\text{-Ala})_2]$
 (B) the equivolume mixture of the 1.00×10^{-2} mol/l solutions of $[\text{Cu}(\text{en})_2]^{2+}$ and $[\text{Cu}(\text{dmga})_2]$

whether or not this ESR method is effective for the identification of two or more complex species in the solution depends upon the degree of separation between the absorption lines of different complex species, their line widths, and the value of K . If the K value is more than about 20, the identification of the parent complexes seems to be almost impossible for solutions with such broad line widths and such small line separations as those shown in Figs. 1—3.²⁰

Symmetry of Ligand Field. When the three principal g values are designated in the order of increasing magnitude as g_1 , g_2 , and g_3 , the axial symmetry of ligand field means that $g_1 = g_2 < g_3$. All the observed ESR spectra of mixed-ligand complexes were similar to each other in absorption line shape, as the several ESR spectra shown in Figs. 1—3 show; they all have an intense absorption line in the high-field part and three or four very weak absorption lines in the low-field part. It can be concluded from a theoretical consideration of the ESR line shape that the copper(II) complexes showing this type of line shape are of axial or near axial symmetry in the ligand field; all the mixed-ligand complexes dealt with in this study are approximately square-planar (tetragonal) complexes in a solution.^{18,19}

When the g values at the positions of the two circles in Figs. 1 and 3 are designated as g' and g'' , whose values are listed in Tables 2 and 3, these g values may be used as a measure in comparing the symmetry of the ligand field between the mixed-ligand complexes and the parent complexes, although this method of comparison is accompanied by somewhat complicated factors due to the hyperfine and extra-hyperfine structures.^{17,18}

18) R. H. Sands, *Phys. Rev.*, **99**, 1222 (1955); T. Vännegard and R. Aasa, *Proc. 1st Intern. Congr. "Paramagnetic Resonance,"* Jerusalem, 1962, Academic Press, New York (1963), p. 509.

19) R. Neiman and D. Kivelson, *J. Chem. Phys.*, **35**, 156 (1961).

20) H. Yokoi, M. Otagiri, and T. Isobe, *this Bulletin*, **44**, 2402 (1971).

TABLE 2. EXPERIMENTAL RESULTS OF PARENT COMPLEXES

Sample solution ^{a)}	$g_{//}$	$g'^{(b)}$	$g''^{(b)}$	$\frac{-A_{//}}{\times 10^4 \text{ cm}^{-1}}$	$\lambda_{\text{max}} \text{ m}\mu$	$\epsilon_{\lambda_{\text{max}}}$	$k_{//}^2$
I	2.206	1.975	2.071	209	554	66	0.56
II	2.208	1.984	2.057	194	570	146	0.55
III	2.213	1.996	2.045	185	594	192	0.54
IV	2.220	1.984	2.061	199	574	110	0.58
V	2.264	2.015	2.061	181	622	58	0.64
VI	2.267	2.020	2.063	180	628	52	0.64
VII	2.251	2.011	2.061	180	620	110	0.61
VIII	2.285	2.025	2.077	139	636	59	0.68

a) The numbers are the ones referred to in Table 1.

b) These g values correspond to the ones at the positions shown in Figs. 1 and 3.

TABLE 3. EXPERIMENTAL RESULTS OF MIXED-LIGAND COMPLEXES

Sample solution ^{a)}	No. of mixed-ligand complex	$g_{//}$	$g'^{(b)}$	$g''^{(b)}$	$\frac{-A_{//}}{\times 10^4 \text{ cm}^{-1}}$	$\lambda_{\text{max}}^{\text{c})} \text{ m}\mu$	$\epsilon_{\lambda_{\text{max}}^{\text{c})}}$	$k_{//}^2$
I-II	1	2.210	1.980	2.056	204	561	94	0.57
I-III	2	2.210	1.984	2.050	202	576 (575)	121 (120)	0.55
I-IV	3	2.214	1.981	2.060	206	562	85	0.57
I-V	4	2.235	1.998	2.058	193	586 (590)	60 (64)	0.61
I-VI	5	2.233	1.996	2.055	194	587 (606)	58 (78)	0.60
I-VII ^{d)}	6							
I-VIII	7	2.242	2.006	2.061	184	598 (605)	62 (70)	0.61
II-III	8	2.211	1.990	2.051	188	586	173	0.54
II-IV	9	2.219	1.987	2.063	193	575	124	0.57
II-V	10	2.231	1.961	2.057	195	586	97	0.59
II-VI	11	2.235	1.996	2.058	195	587	89	0.60
II-VII	12	2.230	1.996	2.066	198	591	137	0.59
II-VIII	13	2.238	2.002	2.053	194	600 (607)	101 (105)	0.60
III-IV	14	2.218	1.990	2.057	190	586	134	0.56
III-V	15	2.226	1.996	2.050	199	590	116	0.58
III-VI	16	2.227	1.991	2.057	199	586 (580)	106 (90)	0.58
III-VII	17	2.229	1.993	2.062	195	592	176	0.58
III-VIII	18	2.237	2.022	2.061	194	610	135	0.59
IV-V	19	2.239	1.997	2.057	199	589	80	0.61
IV-VI	20	2.242	1.990	2.057	192	590	75	0.62
IV-VII	21	2.247	2.001	2.057	190	601	105	0.62
IV-VIII	22	2.244	2.004	2.058	187	597	83	0.62
V-VI	23	2.266	2.016	2.063	178	625	54	0.64
V-VII	24	2.256	2.012	2.059	181	620	79	0.62
V-VIII	25	2.272	2.016	2.050	158	634 (637)	60 (62)	0.65
VI-VII	26	2.262	2.013	2.061	182	622	73	0.64
VI-VIII	27	2.279	2.020	2.066	158	640	57	0.66
VII-VIII	28	2.262	2.017	2.064	193	633	81	0.62

a) The sample solution of two numbers hyphenated together represents an equivolume mixture of the solutions of the numbers referred to in Table 1.

b) Those g values correspond to the ones at the positions shown in Figs. 1 and 3.c) The numbers in parentheses represent the ones of pure mixed-ligand complexes determined by spectrophotometrical analysis, which will be described in our next paper of this series.²⁰⁾

d) The ESR data could not be obtained for this mixed-ligand complex.

 $\Delta g'$ and $\Delta g''$ are defined as follows:

$$\Delta g' = g'(\text{M}) - g'(\text{P}_s)$$

$$\Delta g'' = g''(\text{P}_1) - g''(\text{M})$$

where $g'(\text{M})$ and $g''(\text{M})$ are the g' and g'' values re-spectively of a mixed-ligand complex, and where $g'(\text{P}_s)$ is the smaller value of the two g 's of its parent complexes, and $g''(\text{P}_1)$, the larger value of the two g 's of the parent complexes. This, therefore, means that if $\Delta g' > 0$ and $\Delta g'' > 0$ for a mixed-ligand complex, the intense

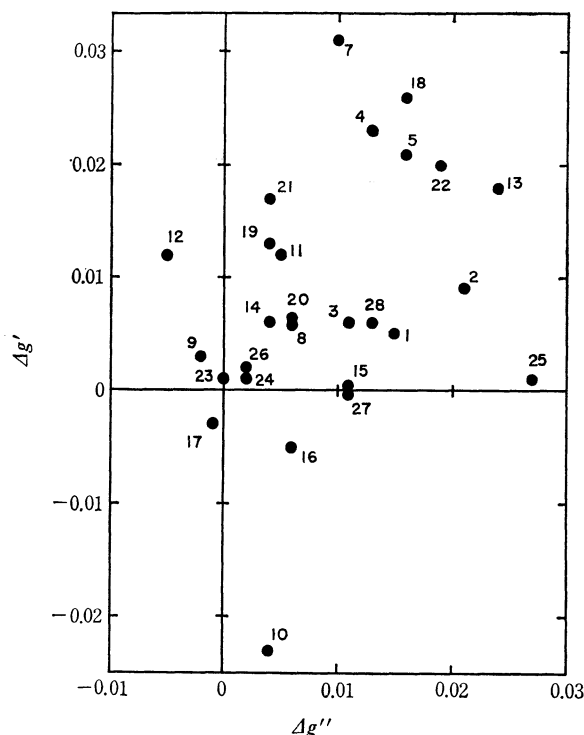


Fig. 5. A plot of $\Delta g'$ against $\Delta g''$ for mixed-ligand complexes (the description of $\Delta g'$ and $\Delta g''$ is given in the text, and the number of each point on the figure is the one referred to in Table 3).

absorption line in the high-field part of the complex appears at a position intermediate between those of its parent complexes. The experimental results are shown in Fig. 5, where most of the mixed-ligand complexes appear in the plus range of both $\Delta g'$ and $\Delta g''$. This fact indicates that the axial symmetry of the ligand field for the mixed-ligand complexes is kept at least in almost the same degree as for their parent complexes. This result is also supported by the intensity data of the visible absorption spectra. As may be seen in Tables 2 and 3, the $\epsilon_{\lambda_{\max}}$ values of almost all the mixed-ligand complexes were intermediate between those of the corresponding two parent complexes, and none of the sample solutions had abnormal band widths; the dipole strengths of transition of the mixed-ligand complexes were intermediate between those of the parent complexes. The details will soon be published elsewhere. This spectral fact suggests that the mixed-ligand complexes are not much lower in the symmetry of their ligand fields than are the parent complexes, since it has generally been believed that the intensity of the visible absorption spectrum of a copper(II) complex always increases as the symmetry of the ligand

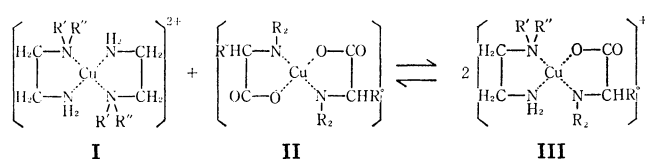


Fig. 6. A schematically represented example of the equilibrium of Eq. (1).

TABLE 4. SYMMETRY

Copper-(II) complex ^{a)}	Coordination groups	Assumed ligand field	Actual ligand field ^{b)}
I	D_{2h}	D_{2h}	near axial
II	D_{2h}	D_{2h}	near axial
III	no symmetry	no symmetry	near axial

a) The numbers of the copper(II) complexes are the ones referred to in Fig. 6.

b) Judged from the observed ESR line shapes.

field of the complex descends.^{21,22)}

When a typical representative example of Eq. (1) is schematically shown in Fig. 6, therefore, the symmetries of the coordinating groups and ligand field for each of the complexes in it can be expressed as is shown in Table 4. Accordingly, the symmetry of the ligand field does not coincide with the apparent symmetry of the coordinating groups, and the symmetry of the ligand field of the planar copper(II) complexes seems to be kept in a high degree, regardless of the different kinds of coordinating groups.

$g_{//}$ and $A_{//}$. According to the ligand field theory of a tetragonal copper(II) complex (D_{4h} symmetry assumed), the following antibonding molecular orbitals, in the order of increasing energy, can be formed for the "hole" configuration²³⁻²⁵⁾:

$$\phi_{b_{1g}} = \alpha d_{x^2-y^2} - \alpha' \phi_L(x^2-y^2) \quad (3)$$

$$\phi_{b_{2g}} = \beta_1 d_{xy} - \beta_1' \phi_L(xy)$$

$$\phi_{a_{1g}} = \alpha_1 d_{z^2} - \alpha_1' \phi_L(z^2)$$

$$\phi_{e_g} = \begin{cases} \beta d_{xz} - \beta' \phi_L(xz) \\ \beta d_{yz} - \beta' \phi_L(yz) \end{cases}$$

In each of the wavefunctions, the ϕ_L in the second term on the right-hand side represents the ligand orbital which can be mixed with the copper d orbital expressed in the first term. The magnetic parameters can then be expressed approximately as follows:

$$g_{//} = 2 - \frac{8\lambda}{\Delta E_{xy}}(\alpha^2 \beta_1^2 - f_1) \quad (4)$$

$$g_{\perp} = 2 - \frac{2\lambda}{\Delta E_{xz}}(\alpha^2 \beta^2 - f_2)$$

$$A_{//} = P \left[-\frac{4}{7} \alpha^2 - \kappa + (g_{//} - 2) + \frac{3}{7} (g_{\perp} - 2) + f_3 \right] \quad (5)$$

$$A_{\perp} = P \left[\frac{2}{7} \alpha^2 - \kappa + \frac{11}{14} (g_{\perp} - 2) + f_4 \right]$$

where $P = 2\gamma\beta_0\beta_N \langle d_{x^2-y^2} | r^{-3} | d_{x^2-y^2} \rangle$, $\Delta E_{xy} = E_{xy} - E_{x^2-y^2}$, and $\Delta E_{xz} = E_{xz} - E_{x^2-y^2}$, and where f_1 — f_4 are small and almost constant values for a variety of copper(II) complexes ($f_1, f_2 \leq 0.04$, $f_3 \leq 0.03$, and $f_4 \leq 0.005$).^{15,24,25)}

21) C. J. Ballhausen, *Progr. Inorg. Chem.*, **2**, 251 (1960); "Introduction to Ligand Field Theory," McGraw-Hill, New York (1962), p. 180.

22) R. L. Belford and W. A. Yeranov, *Mol. Phys.*, **6**, 121 (1963).

23) K. W. Stevens, *Proc. Roy. Soc. (London)*, **A219**, 542 (1953); J. Owen, *ibid.*, **A227**, 183 (1955).

24) A. H. Maki and B. R. McGarvey, *J. Chem. Phys.*, **29**, 31, 35 (1958).

25) D. Kivelson and R. Neiman, *ibid.*, **35**, 149 (1961).

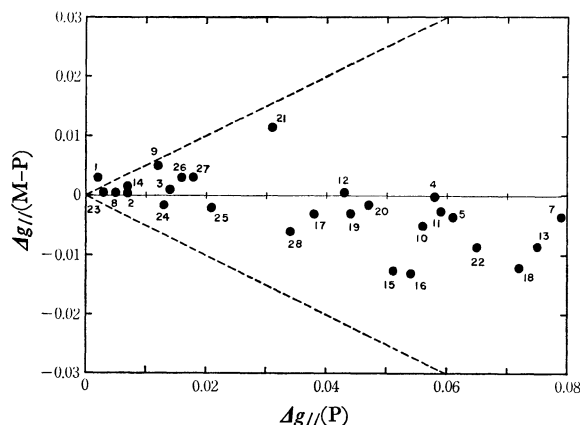


Fig. 7. A plot of $\Delta g_{||}(\text{M-P})$ against $\Delta g_{||}(\text{P})$ for mixed-ligand complexes.

$$\Delta g_{||}(\text{M-P}) = g_{||}(\text{M}) - 1/2(g_{||}^{\text{P}_1} + g_{||}^{\text{P}_2})$$

$$\Delta g_{||}(\text{P}) = |g_{||}^{\text{P}_1} - g_{||}^{\text{P}_2}|$$

where $g_{||}(\text{M})$, $g_{||}^{\text{P}_1}$, and $g_{||}^{\text{P}_2}$ are the $g_{||}$ values of a mixed ligand complex, and its two parent complexes, P_1 and P_2 , respectively. The numbers for the mixed-ligand complexes in Table 3 are employed on this figure.

The experimentally-determined $g_{||}$ and $A_{||}$ values are listed in Tables 2 and 3. The correlation between the $g_{||}$ values of the mixed-ligand complexes and those of the parent complexes is shown in Fig. 7, where, for a mixed-ligand complex, the absolute difference between the $g_{||}$ values of its two parent complexes, $g_{||}^{\text{P}_1}$ and $g_{||}^{\text{P}_2}$, is indicated on the abscissa ($\Delta g_{||}(\text{P})$), and the difference between the $g_{||}$ value of the mixed-ligand complex, $g_{||}(\text{M})$, and the mean of $g_{||}^{\text{P}_1}$ and $g_{||}^{\text{P}_2}$, on the ordinate ($\Delta g_{||}(\text{M-P})$). The dotted lines on this figure express the $g_{||}$ values of two parent complexes against any point of the abscissa. If $\Delta g_{||}(\text{M-P}) = 0$ for a mixed-ligand complex, accordingly, its $g_{||}$ value exactly equals the mean of the two $g_{||}$ values of its parent complexes. This figure clearly shows that the $g_{||}$ values of the mixed-ligand complexes dealt with here are almost equal to the average $g_{||}$ values of the parent complexes.

As to the $A_{||}$ value, a graph was prepared in a similar manner; it is shown in Fig. 8. This figure, however, shows that the points scatter over a considerably wide range, and such a regularity as is indicated for the $g_{||}$

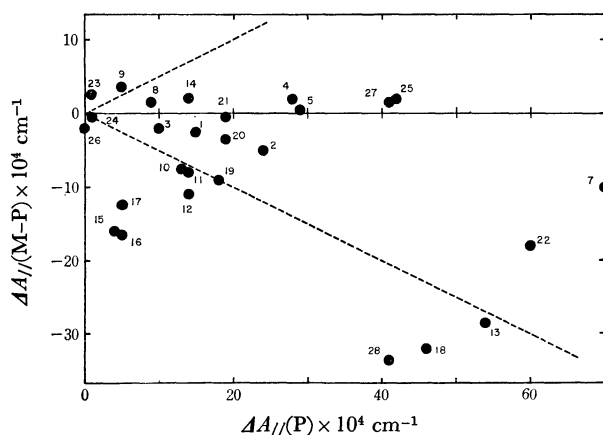


Fig. 8. A plot of $\Delta A_{||}(\text{M-P})$ against $\Delta A_{||}(\text{P})$ for mixed-ligand complexes ($\Delta A_{||}(\text{M-P})$ and $\Delta A_{||}(\text{P})$ are expressed in the similar equations to $\Delta g_{||}(\text{M-P})$ and $\Delta g_{||}(\text{P})$ respectively).

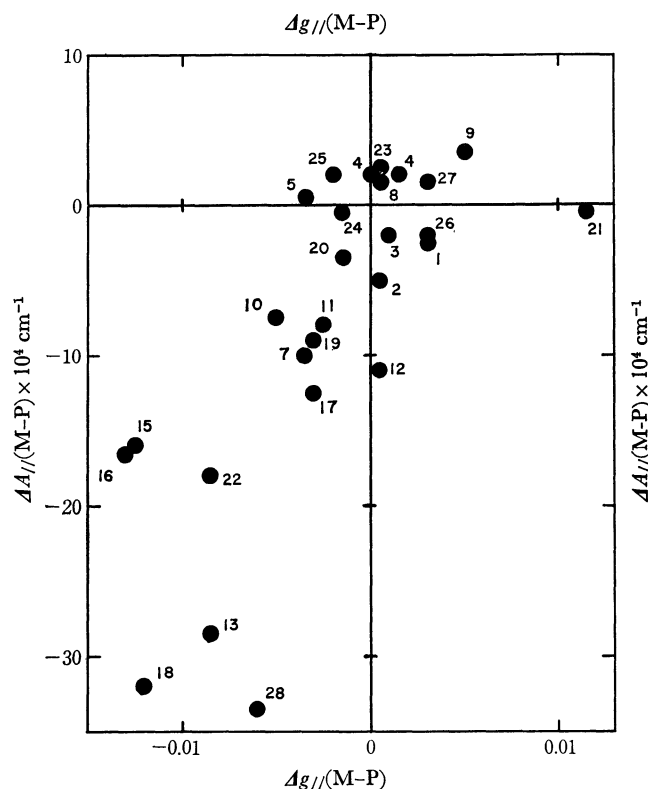


Fig. 9. A plot of $\Delta A_{||}(\text{M-P})$ against $\Delta g_{||}(\text{M-P})$ for mixed-ligand complexes.

value is difficult to find. As an experiment, $\Delta A_{||}(\text{M-P})$ was plotted against $\Delta g_{||}(\text{M-P})$ (cf. Fig. 9). A rough tendency for $\Delta A_{||}(\text{M-P})$ to decrease with the decrease of $\Delta g_{||}(\text{M-P})$ seems to be found in this figure, but this tendency can not be understood only in terms of Eqs. (4) and (5) at the present stage.

Coordination Bonding. At present, the hyperfine parameters are less rigorously related to the structure than are the g values, since the hyperfine parameters depend in complicated ways upon the core spin polarization and, furthermore, upon the $4s$ orbital spin polarization and the p -electron admixture, and since a definite relation between these effects and the covalency of metal-ligand bonds has not yet been established.²⁶⁻³²⁾ It seems, accordingly, that much reliance can not be placed on Eq. (5). The degree of the covalency, therefore, is estimated only from the g values in this work.

Equation (4) is rewritten as follows:

$$g_{||} = 2 - \frac{8\lambda k_{||}^2}{\Delta E_{xy}} \quad (6)$$

26) W. E. Blumberg, "The Biochemistry of Copper," ed. by J. Peisach, P. Aisen, and W. E. Blumberg, Academic Press, New York (1966), p. 49.

27) V. Heine, *Phys. Rev.*, **107**, 1002 (1957); J. H. Wood and G. W. Pratt, *ibid.*, **107**, 995 (1957).

28) B. Bleaney, "Hyperfine interaction," ed. by A. J. Freeman and R. B. Frankel, Academic Press, New York (1967), p. 1.

29) A. J. Freeman, *ibid.*, p. 53.

30) S. Koide, *Phil. Mag.*, **4**, 243 (1959); Y. Tanabe, *Progr. Theoret. Phys. (Kyoto)*, Suppl. **14**, 17 (1960); S. Sugano, *ibid.*, Suppl. **14**, 66 (1960).

31) H. Yokoi and T. Isobe, *This Bulletin*, **39**, 2054 (1966).

32) B. R. McGarvey, *J. Phys. Chem.*, **71**, 51 (1967).

where $k_{//}^2$ is the orbital reduction factor, relating to the bonding parameters, mainly α^2 and β_1^2 . The ligand-field energy of ΔE_{xy} must, then, be estimated in order to determine the value of $k_{//}^2$ from Eq. (6). However, it is not easy to estimate this energy value exactly for the copper(II) complexes with a single broad absorption band in the visible region. Amines and amino acids are arranged in a near position in the spectrochemical series.³³⁾ It seems, therefore, quite likely that all the complexes employed here are similar in the spacing of the energy levels of the d -orbitals. Accordingly, we assumed in this study that the ratio of the energy value of ΔE_{xy} to that of the wavelength of maximum absorp-

tion is almost constant for the complexes. The observed wavelengths of λ_{\max} for all the 1—28 solutions listed in Table 3 except for the 6 and 7 solutions are considered to be nearly equal to those of mixed-ligand complexes themselves, as has been demonstrated in Table 3 by some examples, since the values of K are quite large for those mixed-ligand complexes, which we will discuss in the next paper in this series.²⁰⁾ The above-mentioned assumption is the same as that the energy of λ_{\max} may be directly used in comparing the complexes with each other in terms of the relative values of $k_{//}^2$. The $k_{//}^2$ values thus determined from Eq. (6) for all the mixed-ligand complexes are illustrated graphically in Fig. 10 in a manner similar to that in Figs. 7 and 8. The dotted lines on Fig. 10 also represent the two $k_{//}^2$ values of the parent complexes. It is clear in this figure that most of $k_{//}^2$ values of the mixed-ligand complexes are very close to the mean of the $k_{//}^2$ values of the corresponding parent complexes. It can, furthermore, easily be understood on a simple calculation that, even if the ligand-field energies of the mixed-ligand complexes vary widely from those of the parent complexes, most of the mixed-ligand complexes become intermediate in $k_{//}^2$ value between the parent complexes. Although $k_{//}^2$ is connected with the in-plane bondings, such may be the case with the out-of-plane bondings, judging from the results shown in Fig. 5.

All the above facts suggest that, as to the metal-ligand bonds, the covalency of a mixed-ligand complex is close in degree to the mean of those of the parent complexes. It follows in Eq. (1) that, when the M-A bond is stronger than the M-B bond in the parent complexes, the M-A bond becomes weaker and the M-B bond stronger in the mixed-ligand complex than in the parent complexes; that is, the M-A and M-B bonds become close together in bond strength in a mixed-ligand complex.

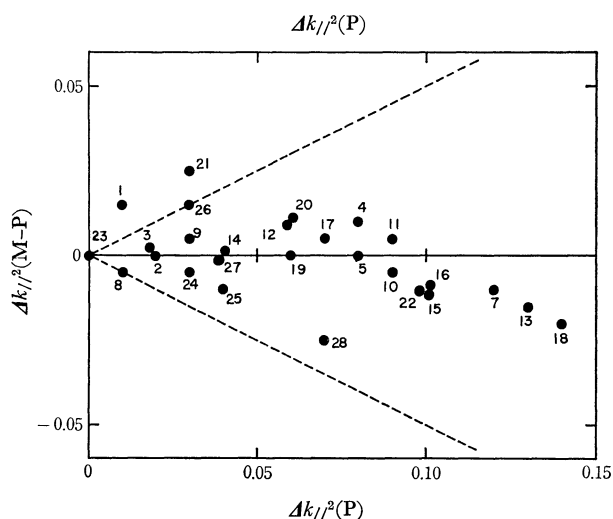


Fig. 10. A plot of $\Delta k_{//}^2(\text{M-P})$ against $\Delta k_{//}^2(\text{P})$ for mixed-ligand complexes ($\Delta k_{//}^2(\text{M-P})$ and $\Delta k_{//}^2(\text{P})$ are expressed in the similar equations to $\Delta g_{//}(\text{M-P})$ and $\Delta g_{//}(\text{P})$ respectively).

33) K. Fajans, *Naturwissenschaften*, **11**, 165 (1923); R. Tsuchida, *This Bulletin*, **13**, 388, 436, 471 (1938).